FAST MODELING OF ACOUSTIC REFLECTIONS AND DIFFRACTION IN COMPLEX ENVIRONMENTS USING VISIBILITY DIAGRAMS

F.Antonacci, M.Foco, A.Sarti, S.Tubaro

DEI - Politecnico di Milano
Piazza L. Da Vinci, 32 - 20133 Milano, Italy

ABSTRACT

In this paper we propose a novel method for computing and auralizing the diffracted field using visibility diagrams. The method allows us to concentrate in a pre-processing phase all the heavy computational tasks that can be performed without knowing the locations of source or receiver. In particular, we can pre-compute the visibility diagrams of all reflectors and all the beam trees (and the corresponding diffracting filters) that are associated to the diffracting wedges on reflectors. Using this information and the source's location, we can generate the corresponding beam tree of geometric reflections. Once the receiver's location is given, we can also generate all geometric paths and the coefficients of the actual diffracting filter. This allows us to model in real-time reflections, diffractions, transmissions in a complex environment with sources and receivers that can freely move.

1. INTRODUCTION

The accurate determination of the sound paths that link source and receiver in complex environments, is a problem of crucial importance in a variety of applications ranging from realistic sound rendering to the modeling of indoor multipath fading in electromagnetic propagation. Several methods have been proposed for a fast determination of such paths. Early approaches, such as ray tracing and image source, were inherited from computer graphics. In the backward ray tracing method a number of rays are cast from the source in all directions and only those that arrive near the receiver end up contributing to the impulse response. A disadvantage of the ray tracing method is a significant risk of omitting relevant paths if we do not trace a sufficient number of rays. Another disadvantage of the ray tracing method is the need to recompute the auralization filter every time either the source or the receiver moves.

Many solutions have been proposed to overcome the above-mentioned limitations. The beam tracing method [2] was developed to partially overcome them. The method is similar to ray tracing, but it is based on the concept of beam (bundle of rays) instead of rays. The idea is to follow the propagation of a beam and to determine how it splits when it encounters a reflecting wall. Since the beam keeps branching out into more sub-beams as it encounters more reflectors on its way, an iterative procedure can be devised and implemented in order to characterize the branching topology. One interesting aspect of this approach is that, given the location of the source, we can pre-compute the branching topology of all beams that propagate from that source through the construction of a data structure called *beam tree*. If we consider a receiver placed in any point in space, we can then quicly determine (through beam-tree lookup) which beams pass through that point and retrieve all the informarmation that is needed to rapidly construct the paths between source and receiver. In conclusion, given a source location, this approach allows us to determine very quickly how the paths change as receiver moves. On the other hand, the beam tree is depends on the reflectors' configuration as well as the source location, therefore every time we move the source, we need to recompute it. This operation can be rather costly, as it needs us to re-evaluate the visibility from the new source location.

A solution to this problem was recently proposed in [3]. The idea behind that method was to first compute the visibility information on the environment (reflectors) from an arbitrary point in space, which is equivalent to the visibility of a generic reflector from a point on a generic relfector. This information is computed and stored in a specific data structure in a preliminary analysis phase. As soon as we specify the source location, we can then iteratively construct the beam tree through lookup of the visibility information. As soon as we specify the receiver's location, we can iteratively determine the paths between source and receiver through beam tree lookup. A clever arrangement of the visibility information based on visibility diagrams (defined in the dual of the geometric space) enables a fast update of the beam-tree, which means that both sources and receivers can move in the environment during the auralization process.

In this paper we propose a method that extends this approach in such a way model diffraction in addition to geometric reflections. In particular, we extend the concept of visibility diagram in order to account for the diffracted field. Diffraction is a fundamental mode of propagation in densely occluded environments. In fact if the source and the receiver are not in direct visibility (and the transmission of sound through walls is negligible), then the first significant acoustic arrival will follow the shortest diffracted path. More generally, the diffracted field tends to enhance the spatial impression of the environment in which the receiver is immersed.

This paper is organised as follows: after a brief description of the adopted model of diffraction (see Section 2), Section 3 will briefly describe the concept of visibility diagram as introduced in [3]. In Section 4 we will illustrate our method for constructing a diffracted beam-tree from visibility information, and we will describe the related auralization process. Section 5 describes a first implementation of the algorithm and illustrates the results of the tests conducted to validate the algorithm.

1.1 Physical models of diffraction

The literature is rich with models that describe diffraction in a more or less physical fashion. Examples of models that are based on a more physical description of the phenomenon are briefly described in [**cite**]. More interesting to us are those models that are based on the Uniform Theory of Diffraction (UTD), which is an extension of the Geometrical Theory of Diffraction (GTD) [1], because they allow us to treat the phenomenon from a purely geometric standpoint. In the UTD

This work was developed within the FIRB-VICOM project (`www.vicom-project.it`) funded by the Italian Ministry of University and Scientific Research (MIUR); and within the VISNET project, a European Network of Excellence (`www.visnet-noe.org`)

the total field is thought of as the superposition of the direct signal (if it exists) and of the field associated to a source positioned on the diffractive wedge. The radiation of this source depends on the angular opening of the wedge, the position of the source and that of the receiver, as well as the considered frequency. A simple expression of the diffracted field as a function of the incident field and the wedge parameters can be found in [5]. In Figure 1, the absolute value of the sum of the diffracted field and of the direct field (where exists) is plotted for various frequencies as a function of the angle between the receiver and the side of the wedge that lies the closest to the source. For the sake of simplicity, we assume the diffractive ridge and the incident ray to be perpendicular. This is quite common in the case of vertical wedges (on walls), when sources and receivers at approximately the same height.

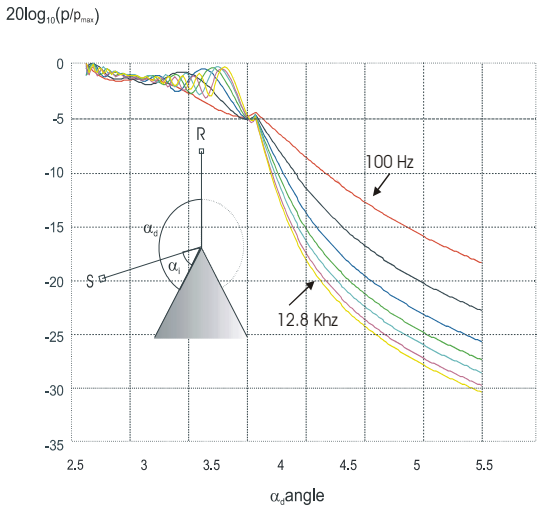

Figure 1: The total normalized field in a frequency range from 100Hz to 12.8Khz as function of the receiver angle α_d with $\alpha_i = \pi/3$.The angle between the source and this side of the wedge is $\pi/4$ and the angular opening of the wedge is also $\pi/4$.

Visual inspection clearly reveals the filtering effect of the diffracted field. In fact, the 100 Hz signal loses 12 dB from a condition in which R is opposite to S at the limit of direct visibility, to a condition in which R lies on the opposite side of the wedge (maximum angle). On the other hand, the 12.8 KHz signal loses 25dB with the same angular shift.

2. VISIBILITY DIAGRAM

In order to illustrate the approach we will assume the space be 2-dimensional.

The first primitive we discuss is the point. It is identified by the coordinates $(\overline{x}, \overline{y})$. The bundle of lines centered on this point has equation $\overline{y} = m\overline{x} + q$, this yields to equation

$$q = -m\overline{x} + \overline{y} \tag{1}$$

In the (m, q) space (also called dual space) this primitive will be represented by a line.

Let us now consider a segment. The segment is determined by his extreme points of coordinates (x_1, y_1) and (x_2, y_2). Using the equation 1 we can easily find the transformation of the two points in the (m, q) space. The segment transformation will be the set of lines included between the two lines corresponding to the extreme points.

The transform of a segment in the (m, q) space is then a beam of lines. In order to obtain the visibility diagram as presented in [3], a rotation, translation and scaling of the axes is done so that the segment s_i (also called the reference segment) falls between the coordinates -1 and 1 on the y axis. The rotation is made so that the virtual source falls in the region where $x \leq 0$. In observance to the image source theorem the beam is not valid in the semispace $x \leq 0$. This task is done for every reflector s_i in our space. In the dual space the segment s_i will be represented by a strip on the q-axis between -1 and 1 and $-\infty \leq m \leq \infty$. The other segments (rotated, translated, scaled in the same manner and eventually cut by the y-axis to respect the image source theorem) transform themselves in a set of bundle of lines. We must now decide an ordering between segments so that when there are superpositions of the duals of the reflectors we can decide which reflectors occlude the other reflectors because in the calculation phase we'll have to divide the beam departing from the segment s_i in beams everyone intersecting only a reflector. The technique of deciding the segments ordering when a superposition takes place is reported in [3]. The visibility diagram ca be thought the ordered collection of reflectors s_j $(j \neq i)$ seen from the s_i segment. In particular for every reference segment we'll create two visibility diagrams: one for each face. This operation, although expensive, can be done in the precalculation phase. An example of a simple visibility diagram will be given in figure 4.

A beam in the (x, y) space is completely determined by his virtual source, the wall that generates it (if exists) and the illuminated region on the wall that limits it (if exists). In the (m, q) space the beam will be then the intersection among the duals of the generator wall, the reflector wall and the virtual source placed behind the generator wall. In this way the dual of a beam in the geometric space will be a line in the (m, q) space. The construction of the beams must be done at calculation time and consists only of a lookup of the pre-existing visibility diagrams.

2.1 Algorithm

The very first phase of the proposed algorithm consists of finding the "diffracting wedges" in the virtual environment. Remembering that the diffracted field gives significant arrivals only in absence of the direct signal, we consider only the wedges with an angular opening (the biggest angle between adjacent segments) bigger than π. In fact (see figure 2) if the angular opening of the wedge is smaller than π and source and receiver reside both in the wedge, the direct signal will be present. If more than two segments converge in a point, the algorithm will find the biggest angle α_w between two adjacent segments. If this angle is bigger than π we'll consider this wedge a diffracting wedge. The described operation can be done in the precalculation phase. Let n_w be the number of wedges in the environment and n_s the mean number of segments converging to the wedge point, the complexity of the algorithm is $n_w n_s \log(n_s)$. In fact, in order to find the adjacent segments we have to consider a segment as a reference segment and the angles the other segments form with this reference segment must be ordered. The ordering algorithm used is the quick-sort whose complexity is just $n_s \log(n_s)$. Also the reflectors that terminate without connecting to other walls are considered diffracting wedges (in this case $\theta = 2\pi$).

The algorithm creates a beam tree for every diffracting wedge we found in the environment. We must decide which depth the "diffracted beam tree" shall assume. This choice is very important to avoid an excessive computation load in the auralizing phase. In fact if the diffracted beam tree has too many nodes, the test could be too expensive. The virtual source will be placed on the edge of each wedge and the first level beams will span as shown in figure 3. If one between

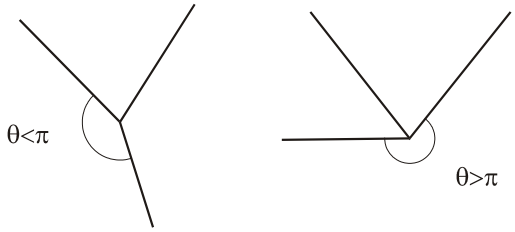

Figure 2: Two examples of wedges: the first isn't a diffracting wedge, the second is a diffracting wedge

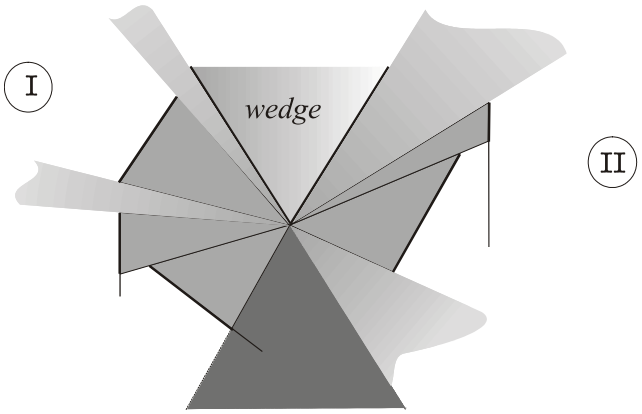

Figure 3: World space and beams departing from the edge of the wedge

receiver and source resides in the dark-grayed zone in figure 3 there will surely be the direct line connecting them and the diffractive signal will not be auralized, while if receiver (source) reside in the zone marked as 1 and source (receiver) reside in the other zone the line of sight signal could be absent. In this case the diffractive beam tree will be tested. On the contrary if receiver and source reside in the same zone we'll not consider the diffracted signal (the line of sight signal or other diffractive paths are present): the beam tree departing from the considered wedge will not be tested. If we place a virtual source on the edge, we must consider the visibility diagram of the first segment that forms the wedge (considering the normalization that moves the segment on the wedge to y-axis between -1 and 1) looking outward the wedge itself. The test operation will be the intersection of this visibility diagram with an horizontal line of equation $q = +1$ or $q = -1$ depending on the sense of rotation used in the normalization of the segment. This line is defined by the interval $m \in (-\infty, m_1)$ or $m \in (m_1, +\infty)$ (see figure 4) depending on the normalization used in the preceding phase. The segments obtained by the intersection of this line with the visibility diagram represent the diffracted beams. The holes between the segments on the q-axis will be filled by infinite beams (marked in the figure 3 with light gray). All these operations can be executed in precalculation phase so that in the calculation phase we'll just have to test these preconstructed beams.

Once the beam tree has been created, we have to render the diffracted field. A naive approach to this problem is the real-time computation of the UTD-filter. Another approach loses some precision in respect to the UTD but tries to eliminate part of its complexity. In fact in most of the applications of virtual acoustics we are more interested in producing a convincing soundtrack than a physically precise

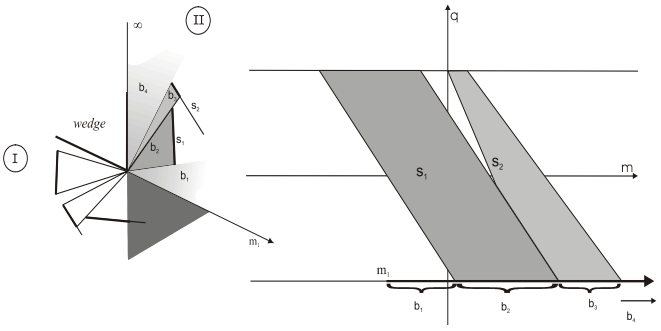

Figure 4: The normalized world space (left) and the visibility diagram of the beams in the beam tree marked as II (right)

one. A simplified method is based on a double interpolation. In particular during the precalculation phase we record the complex value of the diffracted field at the start of the beam (we'll call this position penumbra zone) and under the lee of the wall in shadow (we'll call this position shadow position). This operation is done placing the source at eight angles in the angular range in which the beam tree spans and for eight frequencies between 0 and 3 kHz. The source-wedge and receiver-wedge distances (we need them in the UTD) are assumed to be the mean of the semi-distances between unoccluded walls. We use this information in the calculation phase as follows: we first check that source and receiver reside in the considered beam tree; we calculate then the complex-value of the diffracted field of penumbra and shadow zone as linear interpolation of nearest values in the precalculated structure. The interpolation is angle-based. Given the position of receiver we use a linear angle-based interpolation between the half-light value and shadow value of the diffracted filter to find the value of the frequency response of the diffracting filter at the frequencies we are considering. An inverse Fourier transform is then executed to obtain the required filter.

Called $D_{f,h}(\beta_i)$ and $D_{f,h}(\beta_{i+1})$ the modulus or the phase of the diffracted penumbra field at the two of eight angles nearest the source (whose angle with the nearest side of the wedge is β_s) and at frequency f, the first interpolation is

$$D_{f,h}(\beta_s) \approx D_{f,h}(\beta_i)\frac{\beta_{i+1} - \beta_s}{\beta_{i+1} - \beta_i} + D_{f,h}(\alpha_{i+1})\frac{\beta_s - \beta_i}{\beta_{i+1} - \beta_i} \quad (2)$$

The same interpolation is used with phase and modulus of $D_{f,h}(\beta_s)$.

Analogous relation can be written for phase and modulus of the diffracted field at the shadow zone:

$$D_{f,s}(\beta_s) \approx D_{f,s}(\beta_i)\frac{\beta_{i+1} - \beta_s}{\beta_{i+1} - \beta_i} + D_{f,s}(\beta_{i+1})\frac{\beta_s - \beta_i}{\beta_{i+1} - \beta_i} \quad (3)$$

If now α_r is the angle between the segment composing the wedge nearest the source, $\alpha_1$and α_2 the angles between the same segment anf the start and the end of the lobe in which the receiver resides and using the eq.2 and eq.3, the modulus and phase of the diffracted field at the receiver can be written as follows:

$$D_f(\alpha_r) \approx D_{f,s}(\beta_s)\frac{\alpha_r - \alpha_1}{\alpha_2 - \alpha_1} + D_{f,h}(\beta_s)\frac{\alpha_2 - \alpha_r}{\alpha_2 - \alpha_1} \quad (4)$$

Several other interpolation method could replace this second interpolation. For example it could be observed that the

modulus of the diffracted field is well fitted by a sum of inverse powers of the angle. An example is the following:

$$D_f(\alpha_r) = A_f + \frac{B_f}{\alpha_r} \tag{5}$$

A_f and B_f can be found imposing for example that the start-value of the lobe and the final value of the lobe are fitted by the function at the right member in 5.

Imposing these two conditions we obtain the expressions for A_f and B_f:

$$\begin{aligned} A_f &= D_{f,s}(\beta_s) - \frac{\frac{D_{f,s}(\beta_s) - D_{f,h}(\beta_s)}{1/\alpha_s - 1/\alpha_h}}{\alpha_s} \\ B_f &= \frac{D_{f,s}(\beta_s) - D_{f,h}(\beta_s)}{1/\alpha_s - 1/\alpha_h} \end{aligned}$$

where $D_{f,s}(\beta_s)$ and $D_{f,h}(\beta_s)$ are, respectively, the modulus of the diffracted field at half-light angle (α_h) and at shadow angle (α_s).

The interpolation used to calculate the phase of the diffracted field could be linear. In fact the phase of diffracted field is well fitted by a line.

When the angular opening of the wedge is bigger than $3\pi/2$, the first rendering method should be used. In fact, as shown in the next section, the interpolation method fails.

3. IMPLEMENTATION AND TESTS

The first test we did is the evaluation of the linear interpolation method. The tests results are shown in figure 5.

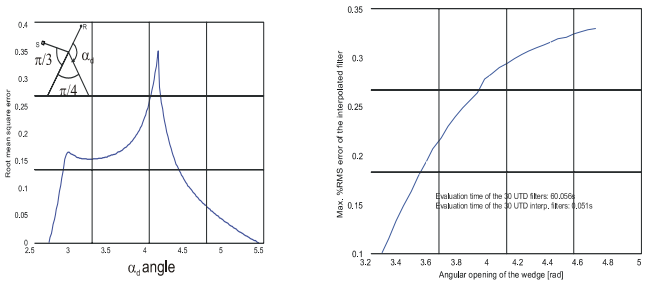

Figure 5: The RMS error of the diffracted filter for a $2\pi - \pi/4$ wedge as function of the receiver angle (left) and the max. RMS error as function of the wedge opening (right)

The first figure displays the RMS error between the interpolated UTD filter and the UTD filter. The RMS error is calculated as follows:

$$E_{RMS}(\alpha_d) = \sqrt{\frac{\sum_n [h_i(n,\alpha_d) - h(n,\alpha_d)]^2}{\sum_n \{\frac{1}{2}[h_i(n,\alpha_d) + h(n,\alpha_d)]\}^2}} \tag{6}$$

In eq. 6 $h_i(n,\alpha_d)$ is the n-th sample of the interpolated filter when the receiver is placed at angle α_d, while $h(n,\alpha_d)$ is the n-th sample of the UTD filter at the same reciever position. In the left-side of figure 5 the wedge opening is $2\pi - \pi/4$ and, as expected, the maximum error takes place when the receiver is in the middle of the diffracted beam. In the implementation a wedge of such an aperture would be auralized by UTD. In the right side of figure 5 is reported the maximum RMS error moving the receiver around the edge for various angles of the wedge itself. As bigger is the angular opening as bigger is the interpolation error. In the same figure are reported the time to calculate the interpolation filters and the UTD filters needed to the test (test executed in Matlab): 0.051s vs. 60s.

The implementation of the above descripted algorithm can be used in two ways: real time and off-line computation. In real-time mode the program computes reflected, transmitted and diffracted paths of the room given receiver and source positions. Also reflections on floor and ceiling (supposed to be constant-height) are considered. Off-line, in addition to the tasks executed in real-time mode, the convolution of the wall-filters encountered between source and receiver is done. In fig.6 the reverberation time at 30dB (for the highlighted environment) using only first-level diffraction beams (right) and without diffraction (left) when source is placed at (-9,2) is reported. The reverberation time can be used as an index of the impulse response length. From a visual inspection of fig. 6 is clear that the length of the impulse response including diffractive paths has increased in occluded areas in comparison with the absence of diffracted field; these zones are marked with circles.

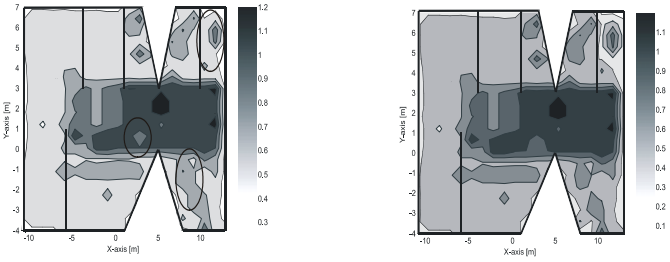

Figure 6: Reverberation time at 30 dB for the higlighted environment with diffraction (left) and without diffraction (right).

REFERENCES

[1] R.G. Kouyoumjian, P.H. Pathak. "A uniform geometrical theory of diffraction for an edge in a perfectly conducting surface ", in *Proc. of IEEE*, November 1974, vol.62, pp. 1448-1461.

[2] T.Funkhouser, I.Carlbom, G.Elko, G.Pingali, M.Sondhi, J.West. "Beam tracing Approach to Acoustic Modeling for Interactive Virtual Environments", *Computer Graphics (SIGGRAPH'98)*, Orlando, FL, July 1998, pp.21-32.

[3] M. Foco, P.Polotti, A.Sarti, S.Tubaro, "Sound spatialization based on fast beam tracing in the dual space", *Proc. of DAFx-03*, London, UK, September 8-11, 2003.

[4] G. Isella, A. Sarti, S. Tubaro, "Efficient geometry-based sound reverberation", *XI European Signal Processing Conference, EUSIPCO 2002*, September 3-6, 2002 Toulouse, France.

[5] N.Tsingos, T.Funkhouser, A.Ngan, I.Carlbom, "Modeling Acoustics in Virtual Environments Using the Unniform Theory of Diffraction", *SIGGRAPH 2001,* August 2001.